

# Bayesian reconstruction of nuclear matter parameters from the equation of state of neutron star matter

Sk Md Adil Imam<sup>1,2</sup>, N. K. Patra<sup>3</sup>, C. Mondal<sup>4</sup>, Tuhin Malik<sup>5</sup>, and B. K. Agrawal<sup>1,2\*</sup>

<sup>1</sup>Saha Institute of Nuclear Physics, 1/AF Bidhannagar, Kolkata 700064, India.

<sup>2</sup>Homi Bhabha National Institute, Anushakti Nagar, Mumbai 400094, India.

<sup>3</sup>Department of Physics, BITS-Pilani, K. K. Birla Goa Campus, Goa 403726, India

<sup>4</sup>Laboratoire de Physique Corpusculaire, CNRS, ENSICAEN, UMR6534, Université de Caen Normandie, F-14000, Caen Cedex, France and

<sup>5</sup>CFisUC, Department of Physics, University of Coimbra, 3004-516 Coimbra, Portugal

(Dated: June 23, 2022)

The nuclear matter parameters (NMPs), those underlie in the construction of the equation of state (EoS) of neutron star matter, are not directly accessible. A Bayesian approach is applied to reconstruct the posterior distributions of NMPs from EoS of neutron star matter. The constraints on lower-order parameters as imposed by the finite nuclei observables are incorporated through appropriately chosen prior distributions. The calculations are performed with two sets of pseudo data on the EoS whose true models are known. The median values of second or higher order NMPs show sizeable deviations from their true values and associated uncertainties are also larger. The sources of these uncertainties are identified as (i) the correlations among various NMPs and (ii) leeway in the EoS of symmetric nuclear matter, symmetry energy, and neutron-proton asymmetry which propagates into the posterior distributions of the NMPs.

## I. INTRODUCTION

The bulk properties of neutron stars are instrumental in constraining the equation of state (EoS) of dense matter [1, 2]. The conditions of charge neutrality and  $\beta$ -equilibrium imposed on the neutron star matter renders it highly asymmetric leading to neutron-proton ratio much larger than unity. The nuclear part of the EoS can be decomposed into two main components: the EoS of symmetric nuclear matter (SNM) and density-dependent symmetry energy. The knowledge of the EoS of neutron star matter may provide an alternative probe to understand the behavior of underlying symmetric nuclear matter and symmetry energy over a wide range of density which may not be readily accessible in the terrestrial laboratory. Usually, the components of neutron star matter EoS are expressed in terms of nuclear matter parameters (NMPs), namely, the energy per nucleon for symmetric nuclear matter, symmetry energy and their density derivatives evaluated at the saturation density ( $\rho_0 \simeq 0.16 \text{ fm}^{-3}$ ). The lower-order NMPs, governing the behavior of neutron star EoS at low densities are determined by nuclear models calibrated to the bulk properties of finite nuclei [3–7]. The higher-order NMPs are generally estimated using observed maximum neutron star mass together with radius and tidal deformability corresponding to the neutron star with canonical mass [8–10]. Such investigations due to the lack of availability of enough experimental data or for sake of simplicity are restricted to a small subspace of NMPs.

Gravitational-wave astronomy through the observations of gravitational wave signals emitted during the merging of binary neutron stars, promises unprecedented constraints on the EoS of neutron star matter. The tidal deformability inferred from these gravitational wave events encodes informa-

tion about the EoS. For the first time, gravitational wave event GW170817 was observed by LIGO-Virgo detector from a low mass compact binary neutron star (BNS) merger with the total mass of the system  $2.74_{-0.01}^{+0.04} M_\odot$  [11, 12]. Another gravitational wave signal likely originating from the coalescence of BNS GW190425 is observed [13]. These two events have already triggered many theoretical investigations to constrain the EoS of neutron star matter [13–22]. The upcoming runs of LIGO-Virgo and the Einstein Telescope are expected to observe many more gravitational wave signals emitted from coalescing neutron stars. The mass and radius of neutron stars, observed either in isolation or in binaries, by the Neutron star Interior Composition Explorer [23–25] have offered complementary constraints on the EoS. A sufficiently large number of such observations may be employed to constrain the NMPs directly which underlie in the construction of the EoS of neutron star matter. Since one needs to estimate simultaneously the values of about ten NMPs, investigations along this direction require computationally efficient statistical tools which allow the evaluation of the likelihood function for the experimental data that may require appropriate marginalization.

A Bayesian approach is often applied to analyze gravitational-wave signals, which involves nearly fifteen parameters, to infer their source properties [26]. It has been also extended to investigate the properties of short gamma-ray burst [27], neutron star [28–30], the formation history of binary compact objects [31–35], population using hierarchical inference [11, 36] and to test general relativity [37–40]. Recently, Bayesian approach has become a useful statistical tool for parameter estimation in the field of nuclear and nuclear astrophysics. It allows one to obtain joint posterior distributions of the model parameters and the correlations among them for a given set of data. Various constraints on the parameters known *a priori* are incorporated through their prior distributions.

Extraction of nuclear matter properties from the chiral effective field theory (EFT), in particular, the issue of over-

\*Electronic address: bijay.agrawal@saha.ac.in

fitting by appropriately choosing the prior is described in great detail in Ref. [41]. Recently, Bayesian techniques have also been employed to constrain symmetry energy [42], masses and radii of neutron stars [43] using the bounds obtained from chiral EFT. To obtain the symmetry energy parameters from lower bound on neutron matter-energy [44]; to extract the crustal properties of neutron star [45, 46]; to limit the bounds on cold neutron star matter EoS from observational constraints [47–49]; to test the compatibility of GW170817 event with multi-physics data [50, 51]; to constrain neutron star matter from existing and upcoming constraints on the gravitational wave and pulsar data [52]; to limit the neutron star EoS with microscopic and macroscopic collisions [53]; to filter models based on astrophysical observations [54]; or to limit the reach of nucleonic hypothesis in the astrophysical context [22, 55] Bayesian techniques have been used extensively.

It is common to study different correlations in the posterior involving parameters and observables alike, within a Bayesian analysis [21, 45, 50, 56]. The origin of these uncertainties is embedded either in the underlying models used or in the variances of the data employed. Existing correlations and uncertainties among the extracted nuclear matter properties from a plethora of nuclear physics data both from the laboratory as well as from the heavens and theoretical calculations at low densities are often left for interpretation [21, 45, 50]. It is also quite useful to test the limit of a certain type of data on physical quantities which are extracted by employing Bayesian analyses. How far the constraints on the static properties of a neutron star can pinpoint the nuclear matter parameters is still a question of great interest. The same applies to the data from heavy-ion collisions which can probe nuclear matter at supra saturation densities [57–59]. These studies can be done only in a controlled environment, as the present observations associate large uncertainties on the data. We have tried to do this by employing theoretical modeling to mimic data on neutron star matter, as well as symmetric matter and symmetry energy.

We first build the EoS of the neutron star matter by expanding it around symmetric nuclear matter within the quadratic approximation as most commonly employed. The EoS of symmetric nuclear matter and density-dependent symmetry energy, the two main components, are further expanded around saturation density within the Taylor and  $\frac{n}{3}$  expansions. The expansion coefficients in the former case are the individual NMPs and their linear combinations in the latter case. A suitable set of NMPs is chosen so that the resulting neutron star matter EoS is consistent with the currently observed maximum mass of  $\sim 2M_{\odot}$  and satisfies the causality condition. As test cases, we employ these EoSs as pseudo data in a Bayesian analysis. The true values of NMPs for the pseudo data are thus known *a priori*. The constraints imposed on the lower-order nuclear matter parameters by the experimental data, for the bulk properties of finite nuclei, are incorporated through appropriate choice of the prior distributions. The median values of marginalized posterior distributions of NMPs and the associated uncertainties on them as obtained for both the EoS models show similar trends. The inherent nature of the model

responsible for the deviations in the median values of NMPs from their true values and uncertainties on them has been identified.

The paper is organized as follows, The Taylor and  $\frac{n}{3}$  expansions for the EoS of neutron star matter are briefly outlined in Sec. II. a Bayesian approach is also discussed in the same section. The results for the posterior distributions of NMPs obtained from the EoS of symmetric nuclear matter, density-dependent symmetry energy and the EoS of neutron star matter is presented in Sec. III. The main outcomes of the present investigation are summarized in the last section.

## II. METHODOLOGY

The nuclear part of the energy per nucleon for neutron star matter  $\varepsilon(\rho, \delta)$  at a given total nucleon density,  $\rho$  and asymmetry,  $\delta$  can be decomposed into the energy per nucleon for the SNM,  $\varepsilon(\rho, 0)$  and the density-dependent symmetry energy,  $J(\rho)$  in the parabolic approximation as,

$$\varepsilon(\rho, \delta) = \varepsilon(\rho, 0) + J(\rho)\delta^2 + \dots, \quad (1)$$

where,  $\delta = \left(\frac{\rho_n - \rho_p}{\rho}\right)$  with  $\rho_n$  and  $\rho_p$  being the neutron and proton densities, respectively. The value of  $\delta$  at a given  $\rho$  is determined by the condition of  $\beta$ -equilibrium and the charge neutrality. Once  $\delta$  is known, the fraction of neutron, proton, electron, muon can be easily evaluated. In the following, we expand  $\varepsilon(\rho, 0)$  and  $J(\rho)$  appearing in Eq. (1) using Taylor and  $\frac{n}{3}$  expansions. The coefficients of expansion in case of the Taylor correspond to the individual nuclear matter parameters. In the latter case, they are expressed as linear combinations of the nuclear matter parameters. These EoSs are used as pseudo data in a Bayesian approach to reconstruct the posterior distributions of nuclear matter parameters.

### A. Taylor's expansion

The  $\varepsilon(\rho, 0)$  and  $J(\rho)$  can be expanded around the saturation density  $\rho_0$  as [60–64],

$$\varepsilon(\rho, 0) = \sum_n \frac{a_n}{n!} \left(\frac{\rho - \rho_0}{3\rho_0}\right)^n, \quad (2)$$

$$J(\rho) = \sum_n \frac{b_n}{n!} \left(\frac{\rho - \rho_0}{3\rho_0}\right)^n, \quad (3)$$

so that,

$$\varepsilon(\rho, \delta) = \sum_n \frac{1}{n!} (a_n + b_n \delta^2) \left(\frac{\rho - \rho_0}{3\rho_0}\right)^n, \quad (4)$$

where the coefficients  $a_n$  and  $b_n$  are the nuclear matter parameters. We truncate the sum in Eqs. (2) and (3) at 4th order, i.e.,  $n = 0 - 4$ . Therefore, the coefficients  $a_n$  and  $b_n$  correspond to,

$$a_n \equiv \varepsilon_0, 0, K_0, Q_0, Z_0, \quad (5)$$

$$b_n \equiv J_0, L_0, K_{\text{sym},0}, Q_{\text{sym},0}, Z_{\text{sym},0}. \quad (6)$$

In Eqs. (5) and (6),  $\varepsilon_0$  is the binding energy per nucleon,  $K_0$  the incompressibility coefficient,  $J_0$  the symmetry energy coefficient, its slope parameter  $L_0$ ,  $K_{\text{sym},0}$  the symmetry energy curvature parameter,  $Q_0$  ( $Q_{\text{sym},0}$ ) and  $Z_0$  ( $Z_{\text{sym},0}$ ) are related to third and fourth order density derivatives of  $\varepsilon(\rho, 0)$  ( $J(\rho)$ ), respectively. The subscript zero indicates that all the NMPs are calculated at the saturation density.

It may be noticed from Eq. (4) that the coefficients  $a_n$  and  $b_n$  may display some correlations among themselves provided the asymmetry parameter depends weakly on the density. Further, the Eq. (4) may converge slowly at high densities, i.e.,  $\rho \gg 4\rho_0$ . This situation is encountered for the heavier neutron stars. The neutron stars with a mass around  $2M_\odot$ , typically have central densities  $\sim 4 - 6\rho_0$ .

### B. $\frac{n}{3}$ expansion

Alternative expansion of  $\varepsilon(\rho, \delta)$  can be obtained by expanding  $\varepsilon(\rho, 0)$  and  $J(\rho)$  as [65, 66],

$$\varepsilon(\rho, 0) = \sum_{n=2}^6 (a'_{n-2}) \left( \frac{\rho}{\rho_0} \right)^{\frac{n}{3}}, \quad (7)$$

$$J(\rho) = \sum_{n=2}^6 (b'_{n-2}) \left( \frac{\rho}{\rho_0} \right)^{\frac{n}{3}}, \quad (8)$$

$$\varepsilon(\rho, \delta) = \sum_{n=2}^6 (a'_{n-2} + b'_{n-2}\delta^2) \left( \frac{\rho}{\rho_0} \right)^{\frac{n}{3}}. \quad (9)$$

We refer this as the  $\frac{n}{3}$  expansion. It is now evident from Eqs.(7) and (8) that the coefficients of expansion are no-longer the individual nuclear matter parameters unlike in case of Taylor's expansion. The values of the NMPs can be expressed in terms of the expansion coefficients  $a'$  and  $b'$  as,

$$\begin{pmatrix} \varepsilon_0 \\ 0 \\ K_0 \\ Q_0 \\ Z_0 \end{pmatrix} = \begin{pmatrix} 1 & 1 & 1 & 1 & 1 \\ 2 & 3 & 4 & 5 & 6 \\ -2 & 0 & 4 & 10 & 18 \\ 8 & 0 & -8 & -10 & 0 \\ -56 & 0 & 40 & 40 & 0 \end{pmatrix} \begin{pmatrix} a'_0 \\ a'_1 \\ a'_2 \\ a'_3 \\ a'_4 \end{pmatrix}, \quad (10)$$

$$\begin{pmatrix} J_0 \\ L_0 \\ K_{\text{sym},0} \\ Q_{\text{sym},0} \\ Z_{\text{sym},0} \end{pmatrix} = \begin{pmatrix} 1 & 1 & 1 & 1 & 1 \\ 2 & 3 & 4 & 5 & 6 \\ -2 & 0 & 4 & 10 & 18 \\ 8 & 0 & -8 & -10 & 0 \\ -56 & 0 & 40 & 40 & 0 \end{pmatrix} \begin{pmatrix} b'_0 \\ b'_1 \\ b'_2 \\ b'_3 \\ b'_4 \end{pmatrix}. \quad (11)$$

The relations between the expansion coefficients and the NMPs are governed by the nature of functional form for  $\varepsilon(\rho, 0)$  and  $J(\rho)$ . The off-diagonal elements in the above matrices would vanish for the Taylor's expansion of  $\varepsilon(\rho, 0)$  and  $J(\rho)$  as given by Eqs. (2) and (3), respectively. Therefore,

each of the expansion coefficients are simply the individual NMPs given by Eqs. (5) and (6). Inverting the matrices in Eqs. (10) and (11) we have,

$$\begin{aligned} a'_0 &= \frac{1}{24}(360\varepsilon_0 + 20K_0 + Z_0), \\ a'_1 &= \frac{1}{24}(-960\varepsilon_0 - 56K_0 - 4Q_0 - 4Z_0), \\ a'_2 &= \frac{1}{24}(1080\varepsilon_0 + 60K_0 + 12Q_0 + 6Z_0), \\ a'_3 &= \frac{1}{24}(-576\varepsilon_0 - 32K_0 - 12Q_0 - 4Z_0), \\ a'_4 &= \frac{1}{24}(120\varepsilon_0 + 8K_0 + 4Q_0 + Z_0), \\ b'_0 &= \frac{1}{24}(360J_0 - 120L_0 + 20K_{\text{sym},0} + Z_{\text{sym},0}), \\ b'_1 &= \frac{1}{24}(-960J_0 + 328L_0 - 56K_{\text{sym},0} - 4Q_{\text{sym},0} \\ &\quad - 4Z_{\text{sym},0}), \\ b'_2 &= \frac{1}{24}(1080J_0 - 360L_0 + 60K_{\text{sym},0} + 12Q_{\text{sym},0} \\ &\quad + 6Z_{\text{sym},0}), \\ b'_3 &= \frac{1}{24}(-576J_0 + 192L_0 - 32K_{\text{sym},0} - 12Q_{\text{sym},0} \\ &\quad - 4Z_{\text{sym},0}), \\ b'_4 &= \frac{1}{24}(120J_0 - 40L_0 + 8K_{\text{sym},0} + 4Q_{\text{sym},0} \\ &\quad + Z_{\text{sym},0}). \end{aligned} \quad (12)$$

Each of the coefficients  $a'$  and  $b'$  are the linear combinations of nuclear matter parameters in such a way that the lower order parameters may contribute dominantly at low densities. The effects of higher-order parameters become prominent with the increase in density.

### C. Bayesian estimation of NMPs

A Bayesian approach enables one to carry out detailed statistical analysis of the parameters of a model for a given set of fit data. It yields joint posterior distributions of model parameters which can be used to study not only the distributions of given parameters but also to examine correlations among model parameters. One can also incorporate prior knowledge of the model parameters and various constraints on them through the prior distributions. This approach is mainly based on the Bayes theorem which states that [67],

$$P(\boldsymbol{\theta}|D) = \frac{\mathcal{L}(D|\boldsymbol{\theta})P(\boldsymbol{\theta})}{\mathcal{Z}}, \quad (14)$$

where  $\boldsymbol{\theta}$  and  $D$  denote the set of model parameters and the fit data. The  $P(\boldsymbol{\theta}|D)$  is the joint posterior distribution of the parameters,  $\mathcal{L}(D|\boldsymbol{\theta})$  is the likelihood function,  $P(\boldsymbol{\theta})$  is the prior for the model parameters and  $\mathcal{Z}$  is the evidence. The posterior distribution of a given parameter can be obtained by marginalizing  $P(\boldsymbol{\theta}|D)$  over remaining parameters. The marginalized posterior distribution for a parameter  $\theta_i$  can be obtained as,

$$P(\theta_i|D) = \int P(\theta|D) \prod_{k \neq i} d\theta_k. \quad (15)$$

We use Gaussian likelihood function defined as,

$$\mathcal{L}(D|\theta) = \prod_j \frac{1}{\sqrt{2\pi\sigma_j^2}} e^{-\frac{1}{2}\left(\frac{d_j - m_j(\theta)}{\sigma_j}\right)^2}. \quad (16)$$

Here the index  $j$  runs over all the data,  $d_j$  and  $m_j$  are the data and corresponding model values, respectively. The  $\sigma_j$  are the adopted uncertainties. The evidence  $\mathcal{Z}$  in Eq. (14) is obtained by complete marginalization of the likelihood function. It is relevant when employed to compare different models. However in the present work  $\mathcal{Z}$  is not very relevant. To populate the posterior distribution of Eq. (14), we implement a nested sampling algorithm by invoking the Pymultinest nested sampler [68] in the Bayesian Inference Library [26].M

### III. BAYESIAN RECONSTRUCTION OF NMPS

We have considered Taylor and  $\frac{n}{3}$  expansions in the previous section to express the EoS for symmetric nuclear matter and the density-dependent symmetry energy in terms of the NMPs. The EoS for neutron star matter can thus be constructed for a given set of NMPs using Eqs. (4) and (9) in a straightforward way. On the contrary, it is not evident that how reliably the values of NMPs can be extracted once the EoS for the neutron star matter is known. To illustrate, we construct EoS for the neutron star matter using Taylor and  $\frac{n}{3}$  expansion for a known set of NMPs. These EoSs are then employed as pseudo data to reconstruct the marginalized posterior distributions of the underlying NMPs through a Bayesian approach. Since the true models for the pseudo data are known, the sources of uncertainties associated with reconstructed NMPs may be analyzed more or less unambiguously. A significant part of the uncertainties on the model parameters usually arises from the intrinsic correlations among them [15, 69]. The intrinsic correlations among the NMPs are the manifestation of the various constraints imposed by the fit data [9, 45]. These correlations may also depend on the choice of forms of the functions for the EoS of symmetric nuclear matter and density-dependent symmetry energy.

#### A. Likelihood function and prior distributions

To obtain the marginalized posterior distributions of model parameters within a Bayesian approach one simply requires a set of fit data, a theoretical model, and a set of priors for the model parameters as discussed in Sec. II C. The likelihood function for a given set of fit data is evaluated for a sample of model parameters populated according to their prior distributions. The joint posterior distributions of parameters are obtained with the help of the product of the likelihood function

and the prior distributions, Eq. (14). The posterior distribution for individual parameters can be obtained by marginalizing the joint posterior distribution with the remaining model parameters. If the marginalized posterior distribution of a parameter is more localized compared to its prior distribution, then, the parameter is said to be well constrained by the fit data.

TABLE I: The values of nuclear matter parameters (in MeV) which are employed to construct various pseudo data using the Taylor and  $\frac{n}{3}$  expansions. The parameters  $\varepsilon_0$ ,  $K_0$ ,  $Q_0$  and  $Z_0$  describes the EoS of the symmetric nuclear matter part and  $J_0$ ,  $L_0$ ,  $K_{\text{sym},0}$ ,  $Q_{\text{sym},0}$  and  $Z_{\text{sym},0}$  describes density-dependent symmetry energy. The index 'N' denotes the order of a given NMP.

N	Symmetric nuclear matter		Symmetry energy	
0	$\varepsilon_0$	-16.0	$J_0$	32.0
1			$L_0$	50.0
2	$K_0$	230	$K_{\text{sym},0}$	-100
3	$Q_0$	-400	$Q_{\text{sym},0}$	550
4	$Z_0$	1500	$Z_{\text{sym},0}$	-750

Our fit data are essentially the pseudo data for the EoS of symmetric nuclear matter, density-dependent symmetry energy, and the EoS for neutron star matter constructed from a suitable choice of NMPs as listed in Table I. The values of lower-order NMPs are close to those obtained from the SLy4 parameterization of the Skyrme force calibrated to the bulk properties for a few selected finite nuclei [70, 71]. The values of second or higher-order NMPs are modified so that the EoS for the neutron star matter remains causal for both the Taylor and  $\frac{n}{3}$  expansions. Further, the maximum mass of neutron stars for both the expansions satisfies the current lower bound of  $\sim 2M_\odot$ . The likelihood function is obtained using Eq (16) for pseudo data and the corresponding model values with the standard deviation,  $\sigma$  equal to unity at all densities ranging from 0.5 -  $6\rho_0$ . The present investigation may not be sensitive to the choice of the NMPs.

TABLE II: Two different sets P1 and P2 for the prior distributions of the nuclear matter parameters (in MeV). The parameters of Gaussian distribution (G) are  $\mu$  (mean) and  $\sigma$  (standard deviation). The parameters 'min' and 'max' denote the minimum and maximum values for the uniform distribution (U). The saturation density  $\rho_0$  is taken to be  $0.16 \text{ fm}^{-3}$ .

Parameters	P1			P2		
	Pr-Dist	$\mu$ min	$\sigma$ max	Pr-Dist.	$\mu$ min	$\sigma$ max
$\varepsilon_0$	G	-16	0.3	G	-16	0.3
$K_0$	G	240	100	G	240	50
$Q_0$	U	-2000	2000	G	-400	400
$Z_0$	U	-3000	3000	U	-3000	3000
$J_0$	G	32	5	G	32	5
$L_0$	U	20	150	G	50	50
$K_{\text{sym},0}$	U	-1000	1000	G	-100	200
$Q_{\text{sym},0}$	U	-2000	2000	G	-550	400
$Z_{\text{sym},0}$	U	-3000	3000	U	-3000	3000

The calculations are performed for two different sets of priors. In Table II, we provide the details for the prior sets P1 and P2. Usually, if the parameters are known only poorly, their prior distribution is taken to be uniform. But, in case, if some information about a parameter is known *a priori*, one simply assumes Gaussian distributions for the corresponding parameter. The priors for  $\varepsilon_0$ , and  $J_0$  are taken to be Gaussian with their means and standard deviations consistent with the constraints imposed by the finite nuclei properties. For most of the remaining NMPs, the prior set P1 assumes uniform distributions. The prior set P2 further imposes stronger constraints on the lower order parameters such as  $K_0$  and  $L_0$  which are consistent with those obtained from finite nuclei properties. The higher-order parameters are assumed to have wide Gaussian distributions. We also impose an additional constraint on the symmetry energy so that it always increases monotonically with density.

### B. Symmetric nuclear matter and symmetry energy

The EoS of the symmetric nuclear matter  $\varepsilon(\rho, 0)$  and the density-dependent symmetry energy  $J(\rho)$  are the two main components which govern the symmetric part and the deviations from it in the EoS of the neutron star matter. The NMPs which are required in the constructions of  $\varepsilon(\rho, 0)$  are  $\varepsilon_0, K_0, Q_0$  and  $Z_0$  and those for  $J(\rho)$  are  $J_0, L_0, K_{\text{sym},0}, Q_{\text{sym},0}$  and  $Z_{\text{sym},0}$ . The nuclear matter parameters that appear in the expansions of  $\varepsilon(\rho, 0)$  might be correlated with those NMPs appearing in the expansion of  $J(\rho)$  (cf Eqs. (4) and (9)). These correlations might prevent the NMPs from being determined accurately. Moreover, the accurate values of NMPs may also be masked by the strong correlations of symmetry energy with the asymmetry parameter  $\delta$  which determines the fractions of different baryons and leptons at a given density. The sources of uncertainties in the NMPs are intrinsically present in a EoS model. To avoid some of these uncertainties, we first consider a Bayesian estimation of the NMPs for a given  $\varepsilon(\rho, 0)$  and  $J(\rho)$  separately, before embarking on their estimations from a EoS of the neutron star matter.

We perform a Bayesian analysis using Gaussian likelihood (cf. Eq. (16)) which can be easily evaluated for a set of fit data together with corresponding model values obtained for a sample of each parameter. We construct two sets of pseudo data for  $\varepsilon(\rho, 0)$  and  $J(\rho)$  each. These pseudo data correspond to the Taylor and  $\frac{n}{3}$  expansions referred hereafter as models M1 and M2, respectively. The values of NMPs used for these pseudo data are the same as listed in Table I. So, the true values of NMPs for a given pseudo data are known. The marginalized posterior distributions (PDs) for the NMPs which underlie in the constructions of  $\varepsilon(\rho, 0)$  and  $J(\rho)$  are obtained separately.

The median values of NMPs and associated  $1\sigma$  uncertainties from the marginalized PDs as listed in Table III are obtained for the models M1 and M2 for two different prior sets. The median values of NMPs obtained for all the different cases are very close to their true values as listed in Table I. The

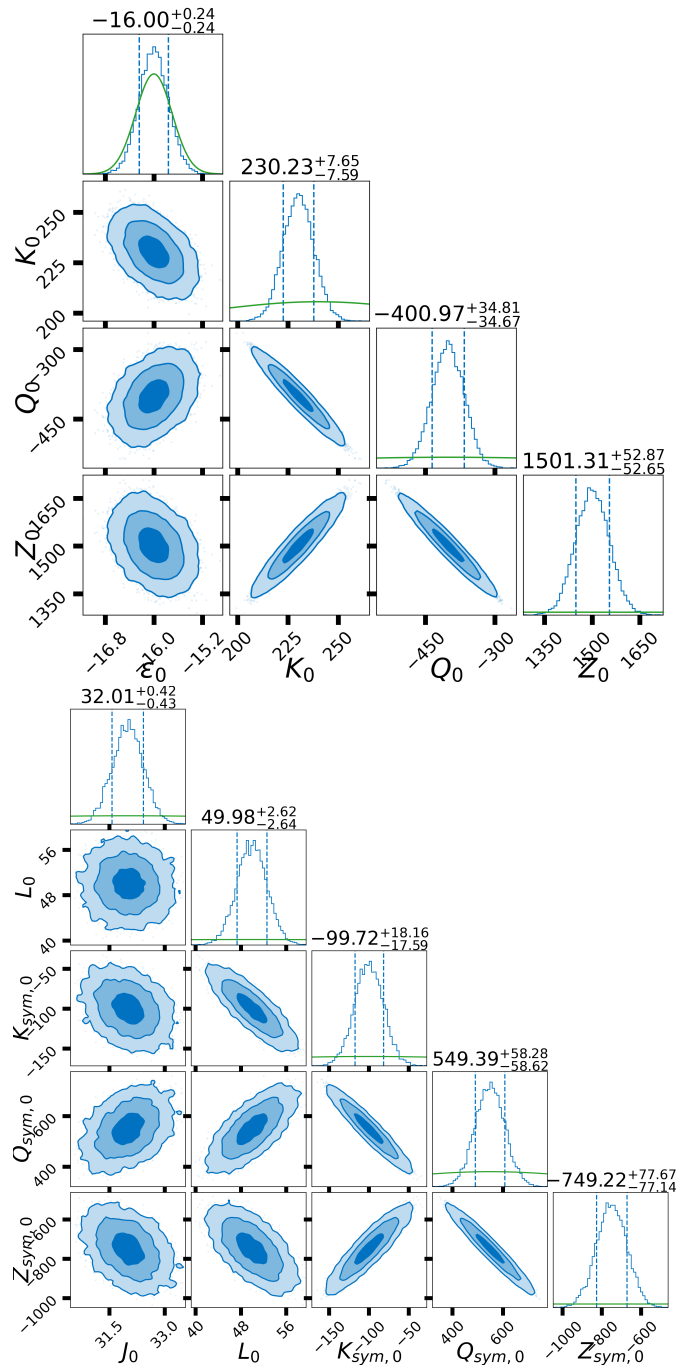


FIG. 1: Corner plots for marginalized posterior distributions of the NMPs which appear in the expansion of the EoS for the symmetric nuclear matter (top) and those in the density-dependent symmetry energy (bottom). The results are obtained for the model M1 with the prior set P2. One dimensional posterior distributions (light blue) plotted along the diagonal plots are also compared with the corresponding prior distributions (light green). The vertical lines indicate the 68% confidence interval of the NMPs. The confidence ellipses for two-dimensional posterior distributions are plotted with  $1\sigma$ ,  $2\sigma$  and  $3\sigma$  confidence intervals.

uncertainties on the NMPs obtained for both the prior sets are quite similar to each other for a given model. However, the uncertainties are significantly larger for the third and fourth-order NMPs in the case of model M2 in comparison to the ones for M1. The uncertainties for third-order NMPs for M2 are about five times larger than those for the M1. It increases to more than ten times for the fourth-order NMPs. The  $1\sigma$  uncertainties obtained from the marginalized PDs for NMPs as listed in Table III are significantly smaller than the ones corresponding to their prior distributions. The prior distribution for a given NMP thus appears relatively uniform compared to their marginalized PD, as will be seen later.

TABLE III: The median values and the  $1\sigma$  errors for the nuclear matter parameters (in MeV) from their marginalized posterior distributions. The distributions of  $\varepsilon_0$ ,  $K_0$ ,  $Q_0$  and  $Z_0$  are reconstructed from the EoS of the symmetric nuclear matter and those for  $J_0$ ,  $L_0$ ,  $K_{\text{sym},0}$ ,  $Q_{\text{sym},0}$  and  $Z_{\text{sym},0}$  from the density-dependent symmetry energy. The results are presented for the Taylor (M1) and  $\frac{n}{3}$  (M2) expansions obtained using prior sets P1 and P2.

NMPs	M1-P1	M1-P2	M2-P1	M2-P2
$\varepsilon_0$	$-16.0^{+0.2}_{-0.2}$	$-16.0^{+0.2}_{-0.2}$	$-16.0^{+0.2}_{-0.2}$	$-16.0^{+0.2}_{-0.2}$
$K_0$	$230^{+8}_{-8}$	$230^{+8}_{-8}$	$230^{+14}_{-15}$	$230^{+13}_{-14}$
$Q_0$	$-402^{+35}_{-35}$	$-401^{+35}_{-35}$	$-403^{+128}_{-124}$	$-403^{+122}_{-116}$
$Z_0$	$1502^{+53}_{-53}$	$1501^{+53}_{-53}$	$1515^{+756}_{-773}$	$1517^{+711}_{-739}$
$J_0$	$32.0^{+0.4}_{-0.4}$	$32.0^{+0.4}_{-0.4}$	$32.0^{+0.5}_{-0.5}$	$32.0^{+0.4}_{-0.4}$
$L_0$	$50.0^{+2.6}_{-2.8}$	$50.0^{+2.6}_{-2.6}$	$50.0^{+2.6}_{-2.6}$	$50.0^{+2.5}_{-2.5}$
$K_{\text{sym},0}$	$-100^{+18}_{-18}$	$-100^{+18}_{-18}$	$-100^{+27}_{-27}$	$-100^{+24}_{-24}$
$Q_{\text{sym},0}$	$551^{+58}_{-59}$	$549^{+58}_{-59}$	$548^{+184}_{-193}$	$551^{+163}_{-166}$
$Z_{\text{sym},0}$	$-750^{+80}_{-75}$	$-749^{+78}_{-77}$	$-734^{+1064}_{-1034}$	$-759^{+936}_{-906}$

The marginalized PDs and the confidence ellipses for the NMPs, which determine  $\varepsilon(\rho, 0)$  and  $J(\rho)$ , obtained for models M1 and M2 are displayed as corner plots in Figs. 1 and 2. These results correspond to prior set P2 which assumes very wide Gaussian distributions for the higher-order NMPs (see Table II). The one-dimensional marginalized PDs for the NMPs are displayed along the diagonals of the corner plots (light blue full lines) together with the corresponding prior distributions (light green lines). These PDs for all the NMPs are quite symmetric around their median values or they represent Gaussian distribution. The PDs for most of the NMPs are localized compared to the corresponding prior distributions. As a result, the prior distributions for most of the NMPs appear to be flat in comparison to the ones for the marginalized PDs. This is also the reflection of the constraints imposed by the pseudo data. The median values of NMPs are very close to their true values. The confidence ellipses are plotted along with the off-diagonal elements of the corner plots corresponding to  $1\sigma$ ,  $2\sigma$ , and  $3\sigma$  confidence intervals. The

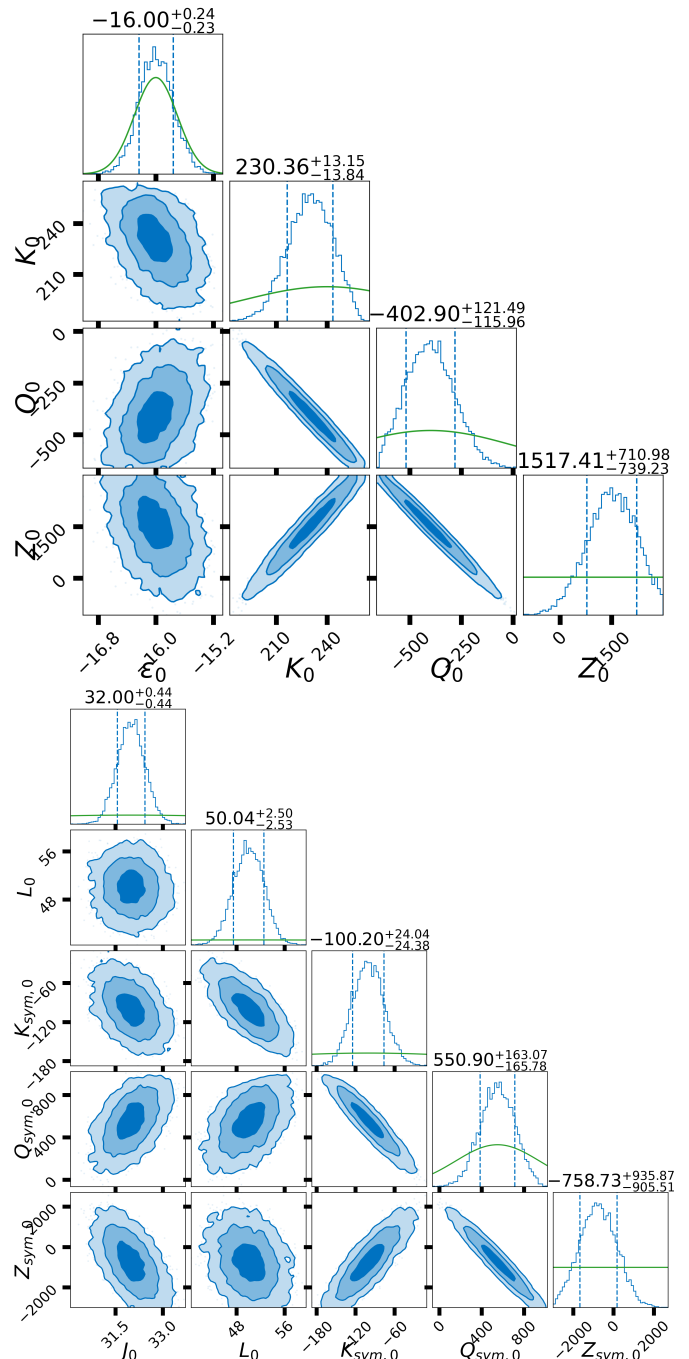


FIG. 2: Same as Fig. 1, but, for model M2.

width and inclination of the confidence ellipses for a pair of NMPs depend on their covariance which determines the nature of the linear correlations among them [69, 72]. It may be noted that the correlation patterns obtained for both models are only marginally different. However, the uncertainties in the higher-order parameters are significantly larger for the model M2. This fact may be attributed to some complex intrinsic correlations among the NMPs. It is clear from Eqs. (12) and (13) that the expansion coefficients for the model M2 are the linear combinations of the NMPs unlike those in M1. Fur-

thermore, it can be seen that the higher-order terms in model M2 relative to the lower-order ones have less impact as compared to those in M1.

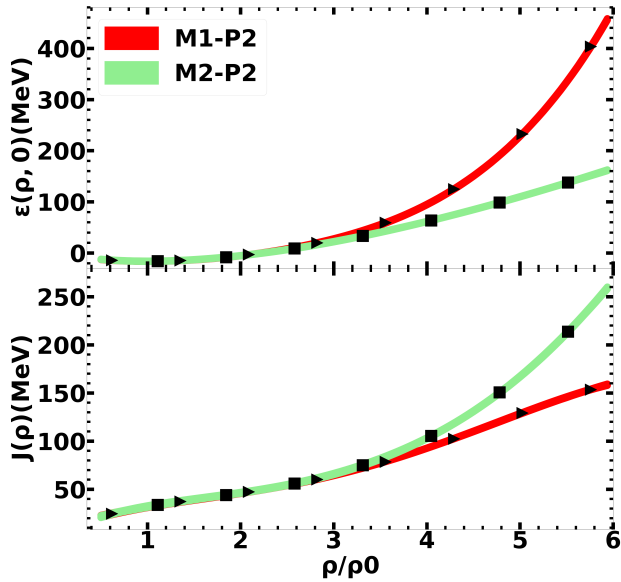


FIG. 3: The EoS for symmetric nuclear matter (top) and the symmetry energy (bottom) as a function of density obtained within 95% confidence interval from the posterior distributions of nuclear matter parameters for models M1 and M2 for the prior set P2. The pseudo data for M1 and M2 are shown by triangles and squares, respectively.

In Fig.3, the variations of  $\varepsilon(\rho, 0)$  and  $J(\rho)$  as a function of density with 95% confidence intervals are plotted. The 95% confidence interval lies in a very narrow range which once again points to the fact that the large uncertainties on the NMPs are predominantly due to the correlations among them. The results presented in Figs. 1-3 provides firm ground to perform the analysis of the NMPs obtained in the following sub-section, using the EoS of neutron star matter, which involves  $\varepsilon(\rho, 0)$  and  $J(\rho)$ , simultaneously. On passing, we may also remark that though the values of  $\varepsilon(\rho, 0)$  and  $J(\rho)$  for the models, M1 and M2 are obtained using the same set of NMPs, their behavior at high densities is significantly different. The lower-order NMPs, which govern the low-density behavior of  $\varepsilon(\rho, 0)$  and  $J(\rho)$ , maybe model-independent.

### C. Neutron star matter

We now apply a Bayesian approach to reconstruct the marginalized PDs for the NMPs using the EoS for the neutron star matter which satisfies the conditions of  $\beta$ -equilibrium and charge neutrality. The EoS for neutron star matter  $\varepsilon(\rho, \delta)$  can be obtained using Eq. (1) for a given  $\varepsilon(\rho, 0)$  and  $J(\rho)$ . We construct two sets of pseudo data for  $\varepsilon(\rho, \delta)$  corresponding to the models M1 and M2 obtained using NMPs of Table I in

Eqs. (4) and (9), respectively. The marginalized distributions of all the nine NMPs are reconstructed simultaneously from the pseudo data for  $\varepsilon(\rho, \delta)$ , since it consists of  $\varepsilon(\rho, 0)$  and  $J(\rho)$ . A Bayesian analysis is performed with models M1 and M2 for prior sets P1 and P2. The median values of the NMPs obtained from the marginalized PDs and the corresponding  $1\sigma$  errors are listed in Table IV. The NMPs are somewhat better estimated for the prior set P2. The symmetry energy slope parameter  $L_0$  seems to be a special case as its counterpart in the symmetric nuclear matter vanishes (cf. Eqs. (5) and (6)). It may be noticed that the uncertainties on  $K_{\text{sym},0}$ ,  $Q_{\text{sym},0}$  and  $Z_{\text{sym},0}$  are much larger than their counterparts in the EoS for symmetric nuclear matter. The errors on  $K_{\text{sym},0}$  are, however, similar to those derived from bulk properties of finite nuclei or other correlation systematics [73–75], though, we have allowed larger variations of  $K_0$  and  $L_0$ . Once, the sufficiently accurate values of  $\varepsilon(\rho, \delta)$  are determined from various astrophysical observations, they can be combined with finite nuclei constraints to obtain  $L_0$  and  $K_{\text{sym},0}$  in tighter limits.

The results for NMPs in Table IV, obtained from the EoS of neutron star matter are substantially different from those of Table III, which were determined separately from the EoS of symmetric nuclear matter and the density-dependent symmetry energy. In general, these differences can be summarized as follows, (i) the median values of NMPs in Table IV show larger deviations from their true values compared to those in Table III, (ii) the uncertainties on the NMPs determined from the EoS of neutron star matter are several times larger for most of the NMPs, (iii) the uncertainties on the  $Z_0$  and  $Z_{\text{sym},0}$  in Table IV are somewhat asymmetric about their median values reflecting their non-Gaussian nature, and (iv) the ratios of uncertainties between the models, M1 and M2 were obtained for third and fourth-order NMPs listed in Table IV are significantly smaller than the ones in Table III. This already provides us some clue that there are additional sources of uncertainties on the NMPs determined from the EoS of the neutron star matter. It may be pointed out that there are several additional sources of uncertainties on the NMPs. It is customary to study different correlations in the posterior involving parameters and observables alike, within a Bayesian analysis. ...Ps which were avoided by reconstructing them separately from the  $\varepsilon(\rho, 0)$  and  $J(\rho)$  as shown in Figs. 1 and 2. These sources of uncertainties are (i) inter-correlations of NMPs corresponding to  $\varepsilon(\rho, 0)$  with the ones for  $J(\rho)$ , (ii) compensation in the change of  $J(\rho)$  with the asymmetry parameter  $\delta$  and  $\varepsilon(\rho, 0)$  in such a way that the EoS of neutron star matter remains more or less unaltered. We analyze them in detail in the following.

The corner plots for the marginalized PDs for the NMPs in one and two dimensions for the models M1 and M2 obtained for prior set P2 are displayed in Figs. 4 and 5, respectively. The difference between the one-dimensional PDs for the NMPs and corresponding prior distributions reflect the role of pseudo data in constraining the NMPs. These marginalized posterior distributions of the NMPs are at variance with those obtained separately from the EoS for the symmetric nuclear matter and the density-dependent symmetry energy as shown in Figs. 1 and 2. The shapes and the orientations of the confidence ellipses suggest that the correla-

TABLE IV: Same as Table III, but, the posterior distributions for all the nuclear matter parameters are reconstructed simultaneously from the EoS for the neutron star matter.

NMPs	M1-P1	M1-P2	M2-P1	M2-P2
$\varepsilon_0$	$-16.0^{+0.3}_{-0.3}$	$-16.0^{+0.3}_{-0.3}$	$-16.0^{+0.3}_{-0.3}$	$-16.0^{+0.3}_{-0.3}$
$K_0$	$187^{+65}_{-56}$	$221^{+36}_{-28}$	$213^{+47}_{-40}$	$230^{+28}_{-25}$
$Q_0$	$-367^{+196}_{-220}$	$-471^{+113}_{-123}$	$-327^{+243}_{-198}$	$-412^{+159}_{-123}$
$Z_0$	$1518^{+258}_{-236}$	$1632^{+152}_{-157}$	$1307^{+1069}_{-1656}$	$1637^{+835}_{-1206}$
$J_0$	$31.8^{+2.5}_{-2.6}$	$32.0^{+2.6}_{-2.7}$	$32.0^{+2.5}_{-2.5}$	$32.0^{+2.6}_{-2.4}$
$L_0$	$52.8^{+25}_{-19}$	$55.5^{+17}_{-16}$	$53.1^{+23.8}_{-19.3}$	$51.0^{+14.0}_{-13.9}$
$K_{\text{sym},0}$	$-34^{+142}_{-178}$	$-108^{+76}_{-72}$	$-114^{+113}_{-138}$	$-106^{+70}_{-70}$
$Q_{\text{sym},0}$	$220^{+755}_{-563}$	$486^{+257}_{-264}$	$562^{+572}_{-488}$	$522^{+248}_{-241}$
$Z_{\text{sym},0}$	$807^{+1341}_{-1527}$	$100^{+876}_{-668}$	$-60^{+1944}_{-1921}$	$-323^{+1920}_{-1643}$

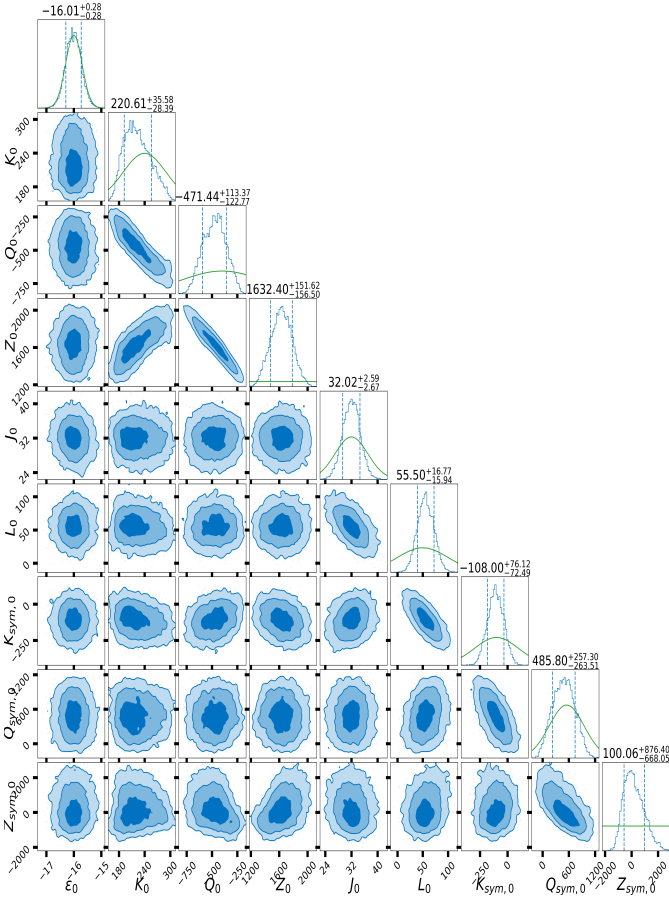


FIG. 4: Corner plots for the marginalized posterior distributions of nuclear matter parameters (in MeV) obtained from the EoS for the neutron star matter for the model M1 with prior set P2. The prior distributions (light green) are also plotted for the comparison.

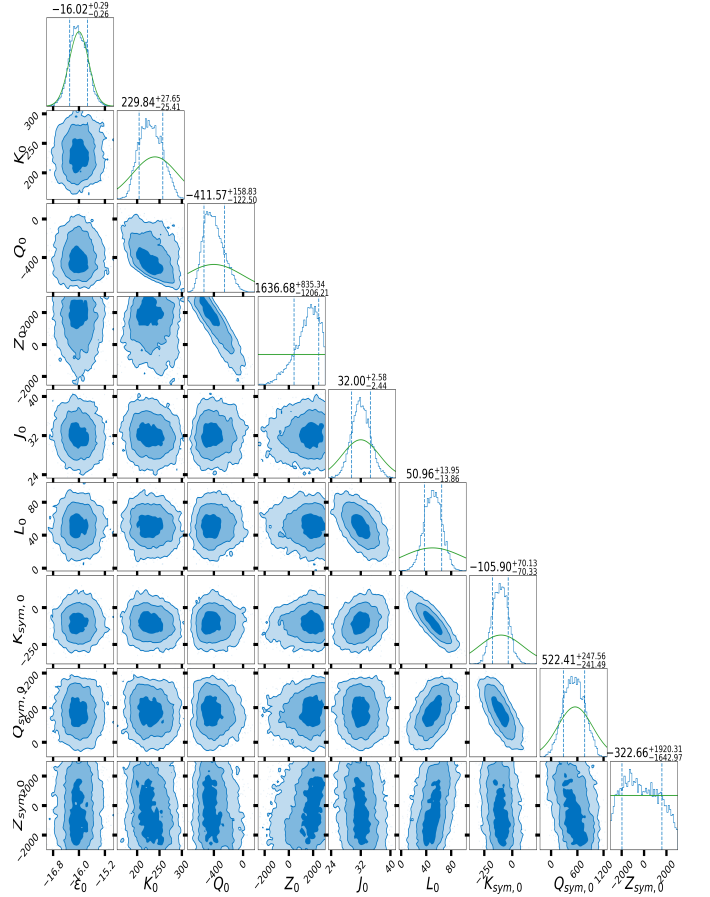


FIG. 5: Same as Fig. 4, but, for the model M2.

tions among most of the pairs of NMPs have disappeared or weakened. Strong correlations exist only between  $K_0 - Q_0$ ,  $Q_0 - Z_0$  and  $L_0 - K_{\text{sym},0}$  pairs with correlation coefficient  $r \sim 0.8$  for model M1. However, in model M2 the  $K_0 - Q_0$  correlation got disappeared. The inter-correlations of the NMPs corresponding to  $\varepsilon(\rho, 0)$  with those for the  $J(\rho)$  are almost absent.  $Z_0$  and  $Z_{\text{sym},0}$  show almost no correlation with the remaining NMPs. Overall reduction in the correlations among the NMPs which are reconstructed from the EoS of the neutron star matter, but, increase in their uncertainties at the same time seem to be somewhat counter-intuitive. Other sources of uncertainties as mentioned earlier need to be addressed.

We now examine the uncertainties in the NMPs which might arise due to the allowed variations in the  $\varepsilon(\rho, 0)$ ,  $J(\rho)$  and  $\delta$  for a given  $\varepsilon(\rho, \delta)$ . The value of asymmetry parameter  $\delta$  is mainly governed by the symmetry energy at a given density. As the symmetry energy increases, the  $\delta$  decreases. Thus, the symmetry energy and  $\delta$  may balance each other in such a way that the asymmetric part of the EoS of neutron star matter remains unaffected. Moreover, the variations in the asymmetric part of  $\varepsilon(\rho, \delta)$  may also be compensated by the symmetric nuclear matter  $\varepsilon(\rho, 0)$ . In short, for a given  $\varepsilon(\rho, \delta)$ , the values of  $J(\rho)$ ,  $\varepsilon(\rho, 0)$  and  $\delta$  may have some leeway. We use the marginalized PDs for the NMPs to obtain 68% and

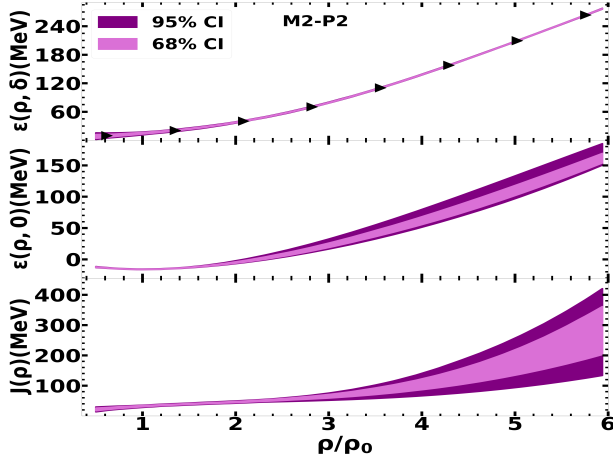


FIG. 6: Plots of 68% and 95% confidence intervals for the EoS for neutron star matter (top), the symmetric nuclear matter (middle), and the symmetry energy (bottom) as a function of scaled density for model M2 with prior set P2. The results are obtained from the posterior distributions of the NMPs which are reconstructed from the pseudo data for the EoS of neutron star matter (triangles). The spread in  $\varepsilon(\rho, 0)$  and  $J(\rho)$  are consistent with those for  $\varepsilon(\rho, \delta)$ .

95% confidence intervals for  $\varepsilon(\rho, \delta)$ ,  $\varepsilon(\rho, 0)$  and  $J(\rho)$ . The results are plotted only for the M2-P2 case in Fig. 6. Other cases show similar qualitative trends and are not shown here. The value of  $\varepsilon(\rho, \delta)$  (top) vary in a narrow bound at a given density, but,  $\varepsilon(\rho, 0)$  (middle) and  $J(\rho)$  (bottom) have larger uncertainties. The 95% confidence intervals for  $\varepsilon(\rho, 0)$  and  $J(\rho)$  are little asymmetric with respect to the ones for the 68% due to the non-Gaussian nature of higher-order NMPs as can be seen from Table IV and Fig. 5. The spread in the values of  $J(\rho)$  increases with density rapidly beyond  $2\rho_0$ . For 68% confidence interval, spread in  $J(\rho)$  at  $4\rho_0$  is  $\sim 36$  MeV which increases to  $\sim 160$  MeV at  $6\rho_0$ , whereas, the spread in  $\varepsilon(\rho, 0)$  remains almost the same ( $\sim 15$  MeV) for the density in the range  $4\rho_0$  to  $6\rho_0$ . The larger spread in  $J(\rho)$  is balanced by asymmetry parameter  $\delta$  as well as by change in  $\varepsilon(\rho, 0)$  such that the EoS for neutron star matter remains almost unaffected. These features are intrinsic in nature which is present in all the models for neutron star matter (cf. Eq. 1). The marginalized PDs for the NMPs, plotted in Figs. 4 and 5 effectively correspond to the values of  $\varepsilon(\rho, 0)$  and  $J(\rho)$  displayed in Fig. 6. To probe further, the confidence ellipses are plotted in Fig. 7 for the 68% confidence intervals for  $\varepsilon(\rho, 0)$ , and  $\delta$  as a function of  $J(\rho)$  at fixed densities  $\rho = 4\rho_0$  and  $6\rho_0$ . The  $J(\rho)$  is anti-correlated with  $\delta$  and  $\varepsilon(\rho, 0)$ . The spread in the values of  $J(\rho)$  is predominantly due to its anti-correlation with  $\delta$ . The uncertainties in  $\varepsilon(\rho, 0)$  and  $J(\rho)$  propagate into the NMPs. That is why, the marginalized posterior distributions of NMPs displayed in Figs. 4 and 5 are significantly different in comparison to those shown in Figs. 1 and 2. This also explains the reason behind the larger uncertainties on the higher-order NMPs, which govern the high-density behavior of  $J(\rho)$ . As

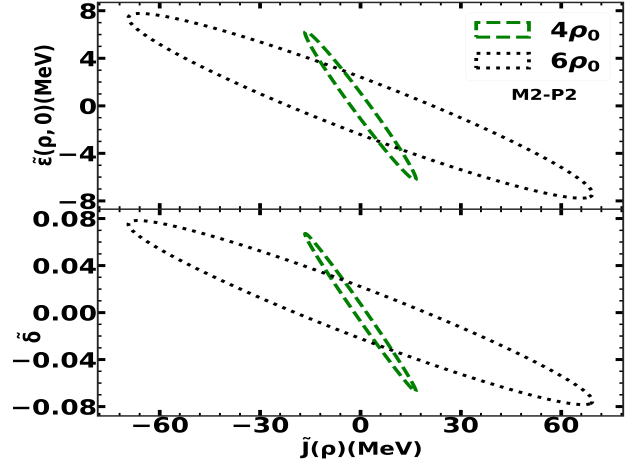


FIG. 7: Plots of confidence ellipses with  $1\sigma$  interval for the EoS for symmetric nuclear matter (top) and asymmetry parameter (bottom) as a function of symmetry energy at densities  $\rho = 4\rho_0$  and  $6\rho_0$ . The symbol tilde denotes that the corresponding quantity is obtained with respect to its median value.

the uncertainties in  $\varepsilon(\rho, 0)$  are smaller than those in  $J(\rho)$ , they get reflected in the uncertainties of the corresponding NMPs (see Table IV). It seems that the EoS of neutron star matter, usually constrained by using several astrophysical observables alone may not be sufficient to determine the NMPs in narrow bounds. The more reliable determination would also require additional constraints on the EoS of symmetric nuclear matter as well as on the density-dependent symmetry energy. The experimental data on the EoS of symmetric nuclear matter from the heavy-ion collision and the symmetry energy beyond the saturation density from the isobaric analog states may help in constraining the NMPs further [76–80].

TABLE V: Values of correlation coefficients among selected pairs of nuclear matter parameters obtained with the modified prior set P2'. The width of Gaussian priors for  $Q_0$  and  $L_0$  are reduced by factor of four and that for  $K_{sym,0}$  by factor of two for P2' in comparison to the prior set P2

Parameters	M1-P2	M1-P2'	M2-P2	M2-P2'
$K_0 - Q_0$	-0.9	-0.75	-0.5	-0.15
$Q_0 - Z_0$	-0.97	-0.87	-0.88	-0.63
$K_{sym,0} - L_0$	-0.76	-0.44	-0.86	-0.62

We modify the prior distributions to simulate the influence of the constraints on the NMPs derived from the data on the microscopic systems such as heavy-ion collisions and the bulk properties of finite nuclei. These data are expected to constrain the behavior of symmetric nuclear matter and symme-

TABLE VI: Same as IV, but, for a modified priors set P2'.

NMPs	M1-P2'	M2-P2'	NMPs	M1-P2'	M2-P2'
$\varepsilon_0$	$-16.0^{+0.3}_{-0.3}$	$-16.0^{+0.3}_{-0.3}$	$J_0$	$32.0^{+2.0}_{-2.0}$	$32.0^{+2.2}_{-2.1}$
			$L_0$	$51.6^{+7.4}_{-7.5}$	$50.0^{+7.2}_{-6.9}$
$K_0$	$212^{+24}_{-21}$	$225^{+27}_{-21}$	$K_{\text{sym},0}$	$-87^{+45}_{-44}$	$-105^{+43}_{-41}$
$Q_0$	$-425^{+63}_{-55}$	$-408^{+62}_{-59}$	$Q_{\text{sym},0}$	$489^{+219}_{-222}$	$544^{+213}_{-209}$
$Z_0$	$1561^{+75}_{-80}$	$1650^{+573}_{-647}$	$Z_{\text{sym},0}$	$-96^{+775}_{-604}$	$-332^{+1857}_{-1621}$

try energy over a wide range of densities ranging from sub saturation density to supra saturation densities up to  $2\text{-}3\rho_0$ . The empirical values of pressure of the symmetric nuclear matter at supra saturation densities may constrain the value of  $Q_0$ . The data on iso-vector giant dipole resonance and neutron-skin thickness in heavy nuclei may constraint the value of  $L_0$  [80]. Once the values of  $J_0$  and  $L_0$  are constrained,  $K_{\text{sym},0}$  may also be somewhat constrained [44, 74]. We repeat our calculations by reducing the width of Gaussian priors for  $Q_0$ ,  $L_0$  and  $K_{\text{sym},0}$  in the prior set P2. For the  $Q_0$  and  $L_0$ , the values of width are reduced by a factor of four, whereas, for the  $K_{\text{sym},0}$  by a factor of two. In Table V, we present the values of correlation coefficients among some selected pairs of NMPs obtained with the modified priors with those for the prior set P2. In general, the correlations become weaker with the modified prior. Consequently, the uncertainties on the NMPs have decreased as can be seen from Table VI. In particular, the uncertainties on  $Z_0$  has now become almost half for both the models M1 and M2. The spread in the values of  $\varepsilon(\rho, 0)$  and  $J(\rho)$  become smaller by less than 10% for the densities around  $2\rho_0$ . But, their spreads at higher densities remain practically unaltered. The issue presented in this paper needs further investigation. In the present work, we have used the most commonly employed EoS expanded around the symmetric nuclear matter. Some alternative representation of the EoS of neutron star matter may be employed. One such form is the expansion of the EoS around the neutron matter in powers of the proton fraction [81].

#### IV. SUMMARY AND OUTLOOK

A Bayesian approach has been applied to reconstruct the underlying nuclear matter parameters which describe the EoS of the neutron star matter. The calculations are performed using the EoS for neutron star matter by expanding it around symmetric nuclear matter within the parabolic expansion as commonly employed. The EoS of symmetric nuclear matter and density-dependent symmetry energy required for such an EoS are expanded using Taylor and  $\frac{n}{3}$  expansions. The expansion coefficients for the former are the individual nuclear matter parameters and the linear combinations of them for the  $\frac{n}{3}$

case. The pseudo data for the EoS for symmetric nuclear matter, neutron star matter, and density-dependent symmetry energy are constructed using both expansions. This pseudo data enable us to identify the various sources of uncertainties associated with the marginalized posterior distributions of NMPs, since, the true models are known. The posterior distributions of the nuclear matter parameters are obtained using two different sets of priors. One of the prior sets assumes that most of the parameters are unknown, except for the lowest order ones which are the binding energy per nucleon for the symmetric nuclear matter and the symmetry energy coefficient at the saturation density.

The marginalized posterior distributions for the NMPs reconstructed separately from the EoS of symmetric nuclear matter and density-dependent symmetry energy are very much localized around their true values. But, the posterior distributions for all the NMPs determined simultaneously from the EoS of neutron star matter are at variance. The median values significantly deviate from their true values and associated uncertainties are also larger, in particular, for second or higher-order NMPs. The main sources of uncertainties are found to be (i) the correlations among higher-order parameters describing the EoS of symmetric nuclear matter and similar correlations in the case of density-dependent symmetry energy and (ii) the larger uncertainties in the symmetry energy at a given density due to its anti-correlation with asymmetry parameter and the EoS of symmetric nuclear matter such that neutron star matter EoS remains mostly unaffected. These are intrinsic in nature for the EoS of neutron star matter obtained by expanding it around the symmetric nuclear matter. The EoS of neutron star matter alone may not be sufficient to determine the higher-order NMPs in narrow bounds. The higher-order NMPs are correlated to the lower-order ones, thus, the low-density ab-initio predictions for the EoS of symmetric nuclear matter and pure neutron matter from the chiral effective field theory should also be considered for the improved parameterizations. The experimental data on the EoS of symmetric nuclear matter from the heavy-ion collision and the symmetry energy beyond the saturation density from the isobaric analog states may further help in constraining the nuclear matter parameters.

We have also performed the calculations by imposing stringent constraints on prior distributions for  $Q_0$ ,  $L_0$  and  $K_{\text{sym},0}$  which led to the reduction of the correlations among the NMPs. Consequently, the uncertainties on some of the NMPs become smaller. The spread in the EoS of symmetric nuclear matter and symmetry energy become smaller by less than 10% for the densities around  $2\rho_0$ . But, their spreads at higher densities remain practically unaltered. It remains to be understood whether the sources of various uncertainties identified in the present work are due to the expansion of the EoS around the symmetric nuclear matter. It may be interesting to perform an investigation using the EoS expanded around the pure neutron matter instead of symmetric nuclear matter[81].

## V. ACKNOWLEDGEMENTS

The authors would like to thank Arunava Mukherjee, Saha Institute of Nuclear Physics for useful discussion, a careful reading of the paper, and important suggestions. N.K.P. would

like to thank T.K. Jha for constant encouragement and support and gratefully acknowledge the Department of Science and Technology, India, for the support of DST/INSPIRE Fellowship/2019/IF190058. C.M. acknowledges partial support from the IN2P3 Master Project “NewMAC”.

- 
- [1] N. A. Webb and D. Barret, *Astrophys. J.* **671**, 727 (2007).  
 [2] J. M. Lattimer and Y. Lim, *Astrophys. J.* **771**, 51 (2013).  
 [3] G. A. Lalazissis, J. König, and P. Ring, *Phys. Rev. C* **55**, 540 (1997).  
 [4] J. Piekarewicz, *Phys. Rev. Lett.* **95**, 122501 (2006).  
 [5] B. K. Agrawal, S. Shlomo, and V. K. Au, *Phys. Rev. C* **72**, 014310 (2005).  
 [6] P. Klupfel, P. G. Reinhard, T. J. Burvenich, and J. A. Maruhn, *Phys. Rev. C* **79**, 034310 (2009).  
 [7] A. Sulaksono, T. J. Bürvenich, P. G. Reinhard, and J. A. Maruhn, *Phys. Rev. C* **79**, 044306 (2009).  
 [8] N.-B. Zhang, B.-A. Li, and J. Xu, *Astrophys. J.* **859**, 90 (2018).  
 [9] B. J. Cai and B. A. Li, *Phys. Rev. C* **103**, 034607 (2021).  
 [10] H. Gil, P. Papakonstantinou, and C. H. Hyun, arXiv:2110.09802, [nucl-th] (2021).  
 [11] B. P. Abbott *et al.*, *Phys. Rev. X* **9**, 011001 (2019).  
 [12] B. P. Abbott *et al.*, *Astrophys. J.* **882**, L24 (2019).  
 [13] B. P. Abbott *et al.*, *Astrophys. J.* **892**, L3 (2020).  
 [14] B. P. Abbott *et al.*, *Phys. Rev. Lett.* **119**, 161101 (2017).  
 [15] T. Malik, N. Alam, M. Fortin, C. Providência, B. K. Agrawal, T. K. Jha, B. Kumar, and S. K. Patra, *Phys. Rev. C* **98**, 035804 (2018).  
 [16] S. De, D. Finstad, J. M. Lattimer, D. A. Brown, E. Berger, and C. M. Biwer, *Phys. Rev. Lett.* **121**, 091102 (2018).  
 [17] F. J. Fattoyev, J. Piekarewicz, and C. J. Horowitz, *Phys. Rev. Lett.* **120**, 172702 (2018).  
 [18] P. Landry and R. Essick, *Phys. Rev. D* **99**, 084049 (2019).  
 [19] J. Piekarewicz and F. J. Fattoyev, *Phys. Rev. C* **99**, 045802 (2019).  
 [20] T. Malik, B. K. Agrawal, J. N. De, S. K. Samaddar, C. Providência, C. Mondal, and T. K. Jha, *Phys. Rev. C* **99**, 052801 (2019).  
 [21] B. Biswas, P. Char, R. Nandi, and S. Bose, *Phys. Rev. D* **103**, 103015 (2020).  
 [22] H. D. Thi, C. Mondal, and F. Gulminelli, arXiv:2109.09675, [astro-ph.HE] (2021).  
 [23] A. L. Watts *et al.*, *Rev. Mod. Phys.* **88**, 021001 (2016).  
 [24] M. C. Miller *et al.*, *Astrophys. J.* **887**, L24 (2019).  
 [25] T. E. Riley *et al.*, *Astrophys. J. Lett.* **887**, L21 (2019).  
 [26] G. Ashton *et al.*, *Astrophys. J. Suppl.* **241**, 27 (2019).  
 [27] S. Biscoveanu, E. Thrane, and S. Vitale, *Astrophys. J.* **893**, 38 (2020).  
 [28] M. W. Coughlin and T. Dietrich, *Phys. Rev. D* **100**, 043011 (2019).  
 [29] F. Hernandez Vivanco, R. Smith, E. Thrane, P. D. Lasky, C. Talbot, and V. Raymond, *Phys. Rev. D* **100**, 103009 (2019).  
 [30] S. Biscoveanu, S. Vitale, and C.-J. Haster, *Astrophys. J.* **884**, L32 (2019).  
 [31] M. E. Lower, E. Thrane, P. D. Lasky, and R. Smith, *Phys. Rev. D* **98**, 083028 (2018).  
 [32] I. M. Romero-Shaw, P. D. Lasky, and E. Thrane, *Month. Not. R. Astron. Soc.* **490**, 5210 (2019).  
 [33] A. Ramos-Buades, S. Husa, G. Pratten, H. Estellés, C. García-Quirós, M. Mateu-Lucena, M. Colleoni, and R. Jaume, *Phys. Rev. D* **101**, 083015 (2020).  
 [34] I. M. Romero-Shaw, N. Farrow, S. Stevenson, E. Thrane, and X. J. Zhu, *Month. Not. R. Astron. Soc.: Lett.* **496**, L64 (2020).  
 [35] M. Zevin, C. P. L. Berry, S. Coughlin, K. Chatziioannou, and S. Vitale, *Astrophys. J.* **899**, L17 (2020).  
 [36] C. Talbot, R. Smith, E. Thrane, and G. B. Poole, *Phys. Rev. D* **100**, 043030 (2019).  
 [37] D. Keitel, *Res. Notes. AAS* **3**, 46 (2019).  
 [38] G. Ashton and S. Khan, *Phys. Rev. D* **101**, 064037 (2020).  
 [39] E. Payne, C. Talbot, and E. Thrane, *Phys. Rev. D* **100**, 123017 (2019).  
 [40] Z. C. Zhao, H. N. Lin, and Z. Chang, *Chin. Phys. C* **43**, 075102 (2019).  
 [41] S. Wesolowski, N. Klco, R. J. Furnstahl, D. R. Phillips, and A. Thapaliya, *J. Phys. G* **43**, 074001 (2016).  
 [42] R. Somasundaram, C. Drischler, I. Tews, and J. Margueron, *Phys. Rev. C* **103**, 045803 (2021).  
 [43] C. Drischler, S. Han, J. M. Lattimer, M. Prakash, S. Reddy, and T. Zhao, *Phys. Rev. C* **103**, 045808 (2021).  
 [44] I. Tews, J. M. Lattimer, A. Ohnishi, and E. E. Kolomeitsev, *Astrophys. J.* **848**, 105 (2017).  
 [45] T. Carreau, F. Gulminelli, and J. Margueron, *Phys. Rev. C* **100**, 055803 (2019).  
 [46] H. D. Thi, T. Carreau, A. F. Fantina, and F. Gulminelli, *Astron. Astrophys.* **654**, A114 (2021).  
 [47] T. E. Riley, G. Raaijmakers, and A. L. Watts, *Month. Not. R. Astron. Soc.* **478**, 1093 (2018).  
 [48] G. Raaijmakers and Others, *Astrophys. J. Lett.* **893**, L21 (2020).  
 [49] J.-L. Jiang, S.-P. Tang, Y.-Z. Wang, Y.-Z. Fan, and D.-M. Wei, *Astrophys. J.* **892**, 1 (2020).  
 [50] H. Güven, K. Bozkurt, E. Khan, and J. Margueron, *Phys. Rev. C* **102**, 015805 (2020).  
 [51] B. Biswas, *Astrophys. J.* **921**, 63 (2021).  
 [52] P. Landry, R. Essick, and K. Chatziioannou, *Phys. Rev. D* **101**, 123007 (2020).  
 [53] S. Huth *et al.*, (2021), arXiv:2107.06229 [nucl-th].  
 [54] B. Biswas, (2021), arXiv:2106.02644 [astro-ph.HE].  
 [55] C. Mondal and F. Gulminelli, (2021), arXiv:2111.04520 [nucl-th].  
 [56] T. Carreau, *Modeling the (proto)neutron star crust : toward a controlled estimation of uncertainties*, Ph.D. thesis (2020).  
 [57] P. Russotto, P. Wu, M. Zoric, M. Chartier, Y. Leifels, R. Lemmon, Q. Li, J. Łukasik, A. Pagano, P. Pawłowski, and W. Trautmann, *Physics Letters B* **697**, 471 (2011).  
 [58] P. Russotto and *et. al.*, *Phys. Rev. C* **94**, 034608 (2016).  
 [59] Adamczewski-Musch and *et. al.* (HADES Collaboration), *Phys. Rev. Lett.* **125**, 262301 (2020).  
 [60] L.-W. Chen, C. M. Ko, and B.-A. Li, *Phys. Rev. C* **72**, 064309 (2005).  
 [61] L.-W. Chen, B.-J. Cai, C. M. Ko, B.-A. Li, C. Shen, and J. Xu, *Phys. Rev. C* **80**, 014322 (2009).  
 [62] W. G. Newton, J. Hooker, M. Gearheart, K. Murphy, D.-H. Wen, F. J. Fattoyev, and B.-A. Li, *Eur. Phys. J. A* **50**, 41 (2014).  
 [63] J. Margueron, R. Hoffmann Casali, and F. Gulminelli, *Phys.*

- Rev. C **97**, 025805 (2018).
- [64] J. Margueron and F. Gulminelli, Phys. Rev. C **99**, 025806 (2019).
- [65] J. M. Lattimer and M. Prakash, Phys. Rept. **621**, 127 (2016).
- [66] H. Gil, P. Papakonstantinou, C. H. Hyun, T.-S. Park, and Y. Oh, Acta Phys. Polon. B **48**, 305 (2017).
- [67] A. Gelman, J. B. Carlin, H. S. Stern, D. B. Dunson, A. Vehtari, D. B. Rubin, J. Carlin, H. Stern, D. Rubin, and D. Dunson, *Bayesian Data Analysis Third edition*, November (CRC Press, 2013).
- [68] J. Buchner, A. Georgakakis, K. Nandra, L. Hsu, C. Rangel, M. Brightman, A. Merloni, M. Salvato, J. Donley, and D. Kocevski, Astron. Astrophys. **564**, 015805 (2014).
- [69] C. Mondal, B. K. Agrawal, and J. N. De, Phys. Rev. C **92**, 024302 (2015).
- [70] E. Chabanat, P. Bonche, P. Haensel, J. Meyer, and R. Schaeffer, Nucl. Phys. A **627**, 710 (1997).
- [71] E. Chabanat, P. Bonche, P. Haensel, J. Meyer, and R. Schaeffer, Nucl. Phys. A **635**, 231 (1998).
- [72] P.-G. Reinhard and W. Nazarewicz, Phys. Rev. C **81**, 051303 (2010).
- [73] C. Mondal, B. K. Agrawal, J. N. De, and S. K. Samaddar, Int. J. Mod. Phys. E **27**, 1850078 (2018).
- [74] C. Mondal, B. K. Agrawal, J. N. De, S. K. Samaddar, M. Centelles, and X. Viñas, Phys. Rev. C **96**, 021302 (2017).
- [75] B. K. Agrawal, T. Malik, J. N. De, and S. K. Samaddar, Eur. Phys. J. Spec. Top **230**, 517 (2021).
- [76] P. Danielewicz, R. Lacey, and W. G. Lynch, Science **298**, 1592 (2002).
- [77] M. B. Tsang, Y. Zhang, P. Danielewicz, M. Famiano, Z. Li, W. G. Lynch, and A. W. Steiner, Phys. Rev. Lett. **102**, 122701 (2009).
- [78] P. Danielewicz and J. Lee, Nucl. Phys. A **922**, 1 (2014).
- [79] C. J. Horowitz, E. F. Brown, Y. Kim, W. G. Lynch, R. Michaels, A. Ono, J. Piekarewicz, M. B. Tsang, and H. H. Wolter, J. Phys. G **41**, 093001 (2014).
- [80] X. Roca-Maza and N. Paar, Prog. Part. Nucl. Phys. **101**, 96 (2018).
- [81] M. M. N. Forbes, S. Bose, S. Reddy, D. Zhou, A. Mukherjee, and S. De, Phys. Rev. D **100**, 083010 (2019).